2021　2022

Investigation of growth dynamics of faceted grain/grain/melt grain boundary
junction during directional solidification of Si

Chuang, Lu-Chung

2,300,000

Experimental methods have been established for studying growth behavior of
grain boundaries (GBs). Symmetric　9 GBs with large deviation, that means high interfacial energy,
were found developing interfacial grooves during solidification. Whereas perfect　9 GBs did not
develop groove at interface.

Findings of this research contribute to the knowledge of interfacial morphology and kinetics of
growing grain boundaries, which are the major defect determining the properties of multicrystalline
materials. Most of the materials in our daily life are multicrystalline.

Crystal growth

Crystal growth　In situ observation　Silicon　Grain boundary　Solid/melt interface

様　式　Ｃ－１９、Ｆ－１９－１、Ｚ－１９（共通）

１．研究開始当初の背景

Grain boundaries (GBs) are two-dimensional defects defining multicrystalline materials. Different types of GBs possess diverse characteristics and their distribution significantly influences the physical properties of multicrystalline materials. GB distribution is mainly formed during solidification, and, therefore, better knowledge of growth behavior of GBs allows for explanation of myriad patterns of GB distribution. For anisotropic crystalline materials, such as Si, GBs develop faceted grooves at solid/melt interface. The growth of GBs with faceted grooves is proposed to be governed by competition of two advancing facets [1]. There are theories explaining twins nucleated at the valley of faceted GB grooves [2, 3]. Proposed theories focused mainly on the growth of two facets and dihedral angles between them. However, a faceted GB groove is a triple junction, which is consisting of two faceted solid/melt interfaces and one GB, as shown in Figure 1. The formation and growth behavior of GB grooves are assumed to be dependent on dynamic equilibrium of the energies of three participating members. In other words, the GB energy must be taken into account for comprehensively explaining the dynamics of growing GB grooves. GB energy is well known dependent on boundary structures. There are some special high angle GBs with low energy called coincidence site lattice (CSL) GBs because of their ordered interfacial structure. Consequently, the GB energy varies hugely across the whole range of misorientation. It is thus necessary to carefully examine the property of GBs participating triple junction during solidification. Most of currently published reports discussed growth behavior of GBs generated randomly during solidification. The lack of studies on well-arranged GBs is because of the difficulty in experimental methods. It is not easy to produce GBs with specific misorientation and boundary plane in crystal growth experiments. For a better knowledge in growth dynamics of GBs during solidification, there is a need to study growing GBs with well-defined characteristics.
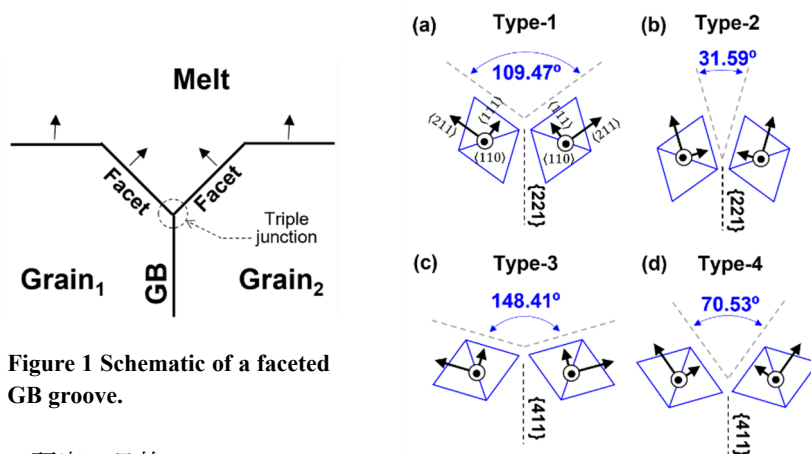

Figure 1 Schematic of a faceted GB groove.

Figure 2 Four possible faceted grooves for Σ9 GBs associated with two symmetric planes, which are {221} and {411}, respectively.

２．研究の目的

In this research, I attempted to investigate that how GB characteristics influences the growth kinetics and nucleation mechanism at the triple junction. I planned to develop new techniques for preparing GBs with acceptable accuracy. Samples with desired GBs will be installed in the crystal growth furnace, which enables in situ observation of the interfacial morphology during directional solidification. The candidate material is Si because it is the most popular semiconductor material and its experimental resources are abundant. The Σ9 GB was chosen as the target of investigation because it is one of the most common GBs in multicrystalline Si. This investigation began with symmetric Σ9 GBs, which possess lower interfacial free energies. With careful arrangement of seeds, two symmetric planes, which are {221} and {411}, associated with four possible faceted grooves are available for experimentation (see Figure 2). The blue diamonds in Figure 2 are the projections of octahedra with faces presenting all eight {111} planes. This experimental setup enables studies of exactly defined triple-junction configurations.

３．研究の方法

Several new experimental methods have been developed for this study, which include seed preparation, method for seed arrangement, modification of the furnace, and treatment for as-grown samples. These methods will be described in detail in the following sections.

(1) Preparation of seeds

The Si wafers of {110} orientation were adopted for preparing the seeds. The wafer was first mounted on a rotating platform with wax. This wafer was rotated by 19.47° counterclockwise, and then cut into two. 19.47° is half of misorientation of a perfect Σ9 GB, which is 38.94° around ⟨110⟩. Two halves were diced into small seeds with a dimension of 5×8 mm. A seed aligned with a flip-over one is able to create a Σ9 GB with a full misorientation of 38.94°. All four triple-junction configurations of interest can be produced in similar ways.

(2) Method for seed arrangement

Two Si seeds aligned side by side were fixed by carbon tape between two quartz plates. A small chip of Si wafer, called feed, was placed next to the seeds. During experiments, the feed will be totally melted. Directional solidification will be started after the melt contacted the seeds.

(3) Modification of the furnace

The temperature control loop of the crystal growth furnace has been modified for better control of temperature gradient and cooling rate. Two thermocouples were installed in the furnace for detection of temperature closer to the sample. Temperature controllers were connected to these two thermocouples enabling measurement with better accuracy. The distance between the tips of two thermocouples is 26 mm, and thus the temperature gradient around the sample can be calculated with temperatures feedbacked by thermocouples. The settings of PID have been optimized allowing for accurate heating and cooling.

(4) In situ observation

The in situ observation system is consisting of a optical microscope and a crystal growth furnace (see Figure 3). The sample set, including seeds, feed, and quartz plates, was put into the furnace between two heaters and two thermocouples (see Figure 4). The temperatures of two heaters were carefully increased to only melt the feed. After the Si melt contacted the seeds, the temperature difference between two thermocouples was adjusted to around 70 K, which gives a temperature gradient of about 2.69 K/mm across the sample. Two heaters were then cooled down simultaneously at a constant rate of -5 K/min. The solid/melt interfacial morphology during directional solidification was observed and recorded by microscope under a well-controlled condition. After the observation, the sample was cooled to room temperature at a rate of -30 K/min.
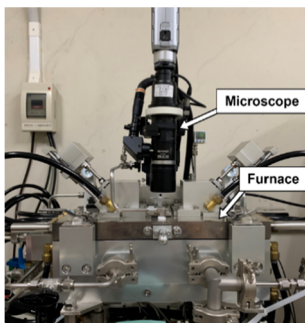

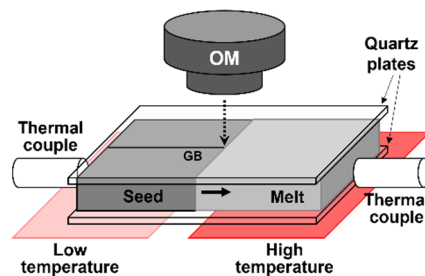**Figure 3 Appearance of in situ observation system.**

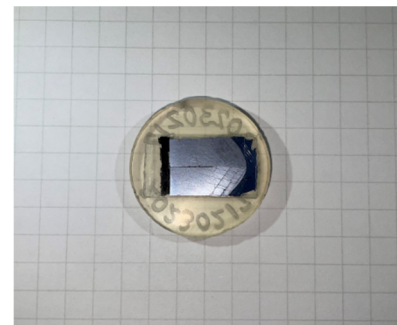**Figure 4 Schematic of the in situ observation system.**

Figure 5 Photo of a sample after the treatment. It is ready for EBSD analysis.

(5) Treatment of as-grown samples

The as-grown samples were mounted in resin immediately after experiments preventing them from breaking into pieces. The mounted samples were then ground and polished to remove quartz plate and create a smooth surface for Si samples. After mechanical polishing, the samples were chemically etched using a HF (46%)-HNO$_3$ (60%) acid mixture with a volume ratio of 1:6 (HF: HNO$_3$) for about 20 s. Figure 5 shows a resin mounted sample after mechanical and chemical polish. Un-melted seeds are on the left side with black carbon tape attached at the edge, and the solidified part extended rightward.

(6) Electron Backscattering Diffraction (EBSD)

The grain orientations and characteristics of GBs of the samples were determined by SEM-EBSD. The sample was tilted by 70° in the SEM chamber. After the electron beams striking the sample surface, a diffraction pattern, known as Kikuchi pattern, was able to be detected by a phosphorus screen installed in the chamber. The orientation of Kikuchi pattern determines the crystalline orientation at each point the electron beam scanned, and thus an orientation map of the sample can be obtained.

(7) Other tests of modified furnace with directional solidification of Ni-Si alloy and Si without seeds

Before performing experiments with seeds, the ability of temperature control of the furnace was tested with non-seeded experiments. Two materials were selected for testing. One material was Ni-Si alloy with a composition of 44% Ni : 56% Si, which is one of eutectic points in Ni-Si binary system. The other material was Si, which would be solidified without seed. Both materials were melted totally in quartz crucibles with inner dimensions of 21 × 13 × 9.5 mm. Specified temperature gradient and cooling rate were set up for demonstrating the furnace's ability of enabling steady directional solidification. The growth processes were started without seeds situ and recorded in situ by an optical microscope.

As-grown Ni-Si blocks were measured by EDS (Energy-dispersive X-ray spectroscopy) to determine

the elemental compositions of the eutectics during solidification; as-grown Si blocks were measured by EBSD for acquiring orientation maps, and the free surface of the Si samples were etched by Sopori etchant to delineate the distribution of lattice dislocations.

4．研究成果

(1) Confirmation of the seed orientation

Before experiments, the orientation of the seeds was checked by EBSD. Two seeds aligned side by side in SEM chamber, and a selected area across the gap between them was chosen for scanning (see Figure 6 (a)). The orientation map (see Figure 6 (b)) shows that the $\Sigma9$ GB, which is type-1, possesses a misorientation of 38.3° around [0 -1 -1]. The deviation is around 0.6° from a perfect $\Sigma9$ GB, which is 38.94° around $\langle110\rangle$. The seeds prepared in this study have a misorientation with high accuracy for following experiments.
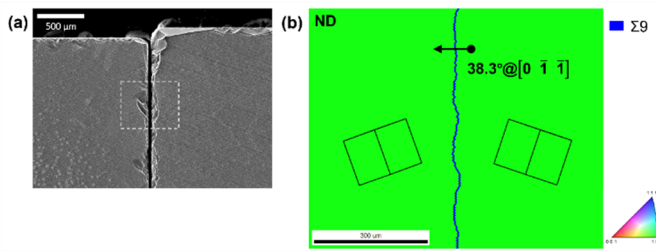

Figure 6 (a) SEM of two seeds aligned side by side. The dashed white rectangle indicates the area scanned by electron beam. (b) Orientation map of scanned area. The misorientation between the two seeds is 38.3° about [0 -1 -1], only 0.6° from a perfect $\Sigma9$. The two black cubes show the orientation of grains with each face presenting all six {100} planes.

(2) In situ observations of type-1, type-3, and type-4 of $\Sigma9$ GBs

During experiments with type-1, type-3, and type-4 $\Sigma9$ GBs, twinning occurred frequently. I couldn't get samples of these $\Sigma9$ GBs without twin nucleation now. Among different nucleated GBs, $\Sigma19a$ GBs were found observed growing stably and developing groove at interface.

(3) In situ observations of type-2 $\Sigma9$ GBs

Samples of type-2 $\Sigma9$ GBs exhibited stability during directional solidification without nucleation. Single growing $\Sigma9$ GBs can be repeatedly obtained. Figure 7 (a) is a snapshot of a selected sample of type-2 $\Sigma9$ GB showing an advancing interface without groove. There was no twinning occurred at this type-2 $\Sigma9$ GB (see Figure 7 (b)). This $\Sigma9$ GB has a deviation of 0.3° from a perfect $\Sigma9$ GB. This GB grew stably over a long distance without developing a groove at the solid/melt interface.

Figure 8 (a) shows a type-2 $\Sigma9$ GB developing a groove at the solid/melt interface. It possesses a higher deviation of 4.8°. This $\Sigma9$ GB was growing steadily with an interfacial groove over a long range. There was no twin GB nucleated at this GB. The pair of $\Sigma3$ GBs below this GB were not nucleated at boundary plane. They were generated at the lower part of the sample, growing upwards, and eventually terminated at this $\Sigma9$ GB. Because these two $\Sigma3$ GBs have opposite misorientations, the boundary structure of the $\Sigma9$ GB will not alter after the interaction with these two $\Sigma3$ GBs. Identical groove still formed at solid/melt interface after the double $\Sigma3$ GBs ran into the $\Sigma9$ GB. The angle of the groove in Figure 8 (a) is about 32.9°, and it is very close to the angle predicted for type-2 $\Sigma9$ GB, which is 31.59° (see Figure 2 (b)).
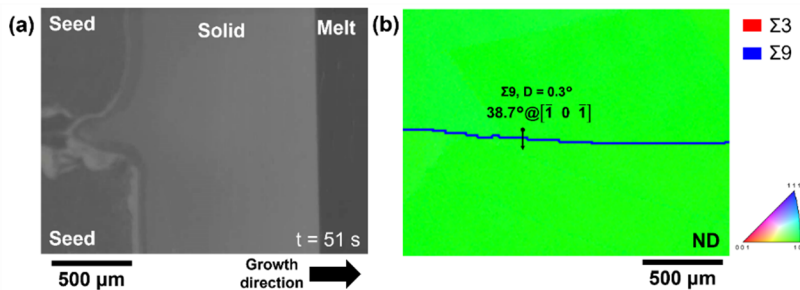

Figure 7 (a) A snapshot taken from in-situ video of advancing solid/melt interface of the second sample of type-2 $\Sigma9$ GB. (b) Orientation map measured by EBSD along normal direction.
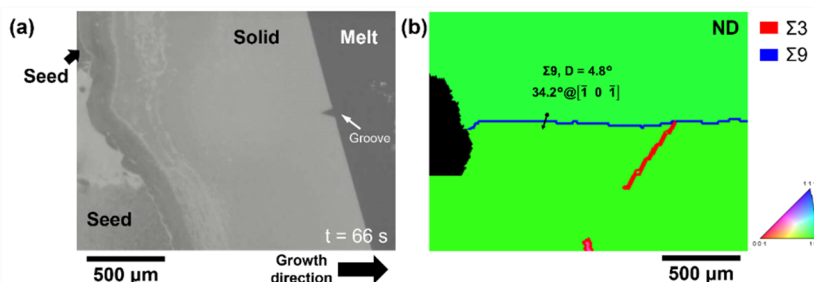

Figure 8 (a) A snapshot taken from in-situ video of advancing solid/melt interface of the third sample of type-2 $\Sigma9$ GB. (b) Orientation map measured by EBSD along normal direction.

(4) Groove formation of type-2 Σ9 GBs

It can be seen clearly that type-2 Σ9 GBs developed no groove at the interface when their deviation was as low as 0.3° (see Figures 7). However, type-2 Σ9 GB with high deviation, which was 4.8° (see Figure 8), developed a groove at the interface. This phenomenon can be explained by considering the boundary structure. CSL GBs, including Σ9 GBs, have atomic coincidence sites at boundary plane, and thus the boundary structure is less mismatched. This is the reason behind lower free energy and relative stability of CSL GBs among high angle GBs. CSL GBs are tolerant to slight deviations by introducing structural defects into boundary plane. Large deviations will introduce disorder into boundary plane, and thus CSL GBs lose their "specialty" and turned into random GBs. There is a method to estimate the extent of CSL GBs' tolerance to deviation. According to Brandon's criterion [4], deviation limit of retaining specialty is able to be estimated by an equation, $\Delta\theta_{max} = 15°/\sqrt{\Sigma}$. $\Delta\theta_{max}$ is the maximum deviation angle for a specific CSL GB, and it varies with Σ values. In the case of Σ9 GBs, $\Delta\theta_{max}$ is 5°. For the type-2 Σ9 GB in Figure 8, its deviation is 4.8°, quite close to the limit defined by Brandon's criterion. This type-2 Σ9 lost the specialty of a Σ9 GB. Its boundary structure was more similar to a random GB, so did its property.

With high deviation, the free energy of a CSL GB became higher. For achieving dynamic equilibrium during directional solidification, the high-energy boundary shrinks and low-energy facets expand. As a result, a faceted groove is thus observed at solid/melt interface. This phenomenon can be explained in a different way. Highly deviated CSL GBs have more mismatched interfacial structure and less bonding between two grains. It suggests that CSL GBs with larger deviation have lower melting point. During directional solidification, the deviated GB fell behind the bulk interface because this two-dimensional defect needs larger undercooling to solidify. The space between the GB tip and the bulk interface is undercooled, and thus two facets formed there, because it is well-known that facets form under undercooled conditions. Both explanations are reasonable, but evidence is not enough to make conclusion. The observed phenomena are summarized in Figure 9.
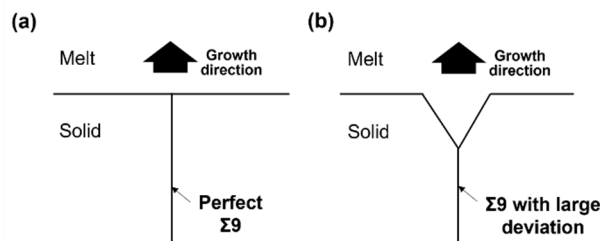

Figure 9 Different interfacial morphologies of a growth type-2 Σ9 GB. (a) A perfect Σ9 GB. It grows without developing a groove. (b) A highly deviated Σ9 GB develops an interfacial

(5) In situ observation of growth of Ni-Si eutectics

Growth of eutectics of $Ni_{44}Si_{56}$ has been successfully observed in situ during directional solidification. The solidification of the eutectic started from the inner wall of the quartz crucible without seeds. Two phases were observed forming at the front of the solid/melt interface. The eutectic of $Ni_{44}Si_{56}$ is a regular eutectic with a typical lamellar structure. Its lamellae spacing λ was determined as 9.8 μm at an average growth rate of 149.6 μm s^{-1}. An interesting phenomenon was found that the lamellae kept evolving during cooling process. The initial densely pack two-phase structure became roughly distributed after the evolution. The two phases were determined by EDS as $NiSi_2$ (primary phase) and $NiSi$ (secondary phase). Both are intermetallics without faceting during directional solidification. The result shows that phase boundaries between these two intermetallics kept migrating actively at a temperature near melting point in solid states. The as-grown eutectic structure is not only influenced by the growth rate, and the cooling process contribute hugely to the final structure in this material. This finding has been published in journal.

(6) Interaction between small-angle GBs and dislocations during directional solidification of Si

(i) Small-angle GBs (SAGBs) with a {111} plane and a misorientation about ⟨111⟩, which means they are twist GBs, are prone to splitting during directional solidification. This type of GBs was observed growing unsteadily along the solidification direction and eventually split and released tons of dislocation afterward. This phenomenon is possibly driven by large stress accumulation at boundary plane of a twist GB. The splitting generates new GBs with less residual stresses.

(ii) SAGBs are acting as dislocation sinks during solidification, especially for grains of smaller sizes. I observed that the misorientations of SAGBs increased after the dislocation clusters disappeared at boundary planes. This finding suggests that SAGBs absorbed lattice dislocations and, consequently, their boundary structure became more disordered.

参考文献
[1] T. Duffar, A. Nadri, *C. R. Phys.* 14 (2013) 185-191
[2] T, Duffar, A. Nadri, *Scr. Mater.* 62 (2010) 955-960
[3] H. K. Lin, C. W. Lan, *Acta Mater.* 131 (2017) 1-10
[4] D.G. Brandon, *Acta Metall.* 14 (1966) 1479-1484

1	1	0	0	
Chuang Lu-Chung Maeda Kensaku Morito Haruhiko Fujiwara Kozo				211
In situ observation of solidification and subsequent evolution of Ni-Si eutectics				2022
Scripta Materialia				114513 114513
DOI 10.1016/j.scriptamat.2022.114513				

5	1	2
Lu-Chung Chuang, Kensaku Maeda, Haruhiko Morito, Kozo Fujiwara		
Small-angle grain boundaries as sinks for lattice dislocations during directional solidification of silicon		
50		
2021		

Lu-Chung Chuang, Kensaku Maeda, Haruhiko Morito, Kozo Fujiwara
Decomposition of small-angle grain boundaries during directional solidification of multicrystalline silicon
11th International Workshop on Crystalline Silicon for Solar Cells (CSSC-11)
2022

Lu-Chung Chuang, Kensaku Maeda, Haruhiko Morito, Kozo Fujiwara
Dislocation generation from small-angle grain boundaries during directional solidification of multicrystalline silicon
The 33rd International Photovoltaic Science and Engineering Conference (PVSEC-33)
2022

0

0